Block copolymer morphologies confined by square-shaped particle: Hard and soft confinement*

Qiyi Zhang(张启义)†, Wenyan Yang(杨文艳), and Kaiyan Hu(胡凯燕)

Department of Mathematics and Physics, Chongqing University of Science and Technology, Chongqing 401331, *China*

(Received 11 May 2016; revised manuscript received 6 July 2016; published online 30 September 2016)

The self-assembly of diblock copolymers confined around one square-shaped particle is studied systematically within two-dimensional self-consistent field theory (SCFT). In this model, we assume that the thin block copolymer film is confined in the vicinity of a square-shaped particle by a homopolymer melt, which is equivalent to the poor solvents. Multiple sequences of square-shaped particle-induced copolymer aggregates with different shapes and self-assembled internal morphologies are predicted as functions of the particle size, the structural portion of the copolymer, and the volume fraction of the copolymer. A rich variety of aggregates are found with complex internal self-assembled morphologies including complex structures of the vesicle, with one or several inverted micelle surrounded by the outer monolayer with the particle confined in the core. These results demonstrate that the assemblies of diblock copolymers formed around the square-shaped particle in poor solvents are of immediate interest to the assembly of copolymer and the morphology of biomembrane in the confined environment, as well as to the transitions of vesicles to micelles.

Keywords: copolymer, square-shaped particle, soft confinement, field theory

PACS: 82.35.Np, 82.35.Jk, 89.75.Fb **DOI:** 10.1088/1674-1056/25/11/118201

1. Introduction

The self-assembly of block copolymers has attracted a great deal of scientific interest due to the formation of various equilibrium ordered structures and the potential applications in biometric technology such as biomaterials, drug delivery, catalysis, sensing, optics and corrosion.[1,2] Diblock copolymers can form various nanostructures in the bulk, including spatially ordered lamellae, bicontinuous cubic phases of gyroids, hexagonal arrays of cylinders, and cubic arrays of spheres.[3–5] It has been demonstrated that confinement is a powerful tool to break the symmetry of a structure, thus allowing materials to form new phases that are not available in bulk systems. In a spatially confined environment, the combination of the structural frustration, confinement-induced entropy loss, and wall interactions provides opportunities to engineer novel structures.[6–17]

In previous studies on confinement-induced morphological transitions, the confining boundaries are flat or curved hard surfaces. This kind of confinement will be termed hard confinement.[18–22] The hard confinement of block copolymers has been examined in many experimental, theoretical, and simulation studies.

On the other hand, in biological systems such as cells, the shape of the confining geometry is not fixed but deformable with the variation of either internal factors or the external environment. In contrast to hard confinement, this kind of confinement can be termed soft confinement.[23] The phase behavior of block copolymers under soft confinement should be richer because the shape of the confining geometry can be changed.

So far, most simulations focused on spherical particles in polymer. However, realistic particles are almost never perfect spheres. For example, the fibers of glass wool, carbon nanotubes, and proteins tend to have more rod-like shapes, whereas most salt crystals are cubic.[24]

In this paper, we will investigate the self-assembly of diblock copolymers under two-dimensional (2D) confinement, where the block copolymers are sandwiched between the square-shaped surface and the homopolymer thin films. In this investigation, we apply numerical self-consistent field theory (SCFT) to study the self-assembly behavior of a diblock copolymer melt confined between the hard surface and the soft surface.

Particularly, self-consistent theory is a powerful method taking into account entropy and enthalpic interaction. Our theoretical understanding can be built based on this well-tested model, which in many ways has provided useful insight into the fusion and fission of a membrane.[25–27]

Despite all the studies in these research fields, the confinement of copolymer at the interface between a hard surface and a soft surface is not found, especially for the square-shaped particle. In this paper, we provide some ideas and conclusions that might be useful on the interactions of vesicles and particles.

*Project supported by the National Natural Science Foundation of China (Grant No. 20804060) and the Research Foundation of Chongqing University of Science and Technology, China (Grant No. CK2013B16).

†Corresponding author. E-mail: qyzhang520@163.com

© 2016 Chinese Physical Society and IOP Publishing Ltd

2. Model and simulation details

Self-consistent field theory (SCFT) has been used successfully over a number of years to model the equilibrium structures formed in melts and blends of polymers[28–30] and may also be used to investigate metastable structures.[25,31,32] Here, the real-space approach scheme introduced by Fredrickson and Drolet[30,33,34] is used to study the assembly structures of an incompressible copolymer–homopolymer mixture. The system consists of n_a linear amphiphilic copolymers and n_s solvent molecules. The amphiphilic molecules are composed of A (hydrophilic) and B (hydrophobic) blocks, and the solvent molecules are represented by hydrophilic homopolymers consisting of A segments only. Each homopolymer and copolymer chain has the same degree of polymerization N with a fixed monomer volume $1/\rho_0$. We assume that the A and B segments have the same segment length b. The volume fraction of the copolymer is specified by f $(0 < f < 1)$. The dimensionless free energy of the system is given by[35–38]

$$\begin{aligned}\frac{NF}{\rho_0 k_B T V} &= -\bar{\phi}_a \ln\left(\frac{Q_a}{V\bar{\phi}_a}\right) - \bar{\phi}_s \ln\left(\frac{Q_s}{V\bar{\phi}_s}\right) \\ &+ \frac{1}{V}\int d\boldsymbol{r}[\chi N\phi_h(\boldsymbol{r})\phi_t(\boldsymbol{r}) + \chi N\phi_s(\boldsymbol{r})\phi_t(\boldsymbol{r})] \\ &- \frac{1}{V}\int d\boldsymbol{r}[(w_h(\boldsymbol{r}) - H(\boldsymbol{r}))\phi_h(\boldsymbol{r}) \\ &+ (w_t(\boldsymbol{r}) - H(\boldsymbol{r}))\phi_t(\boldsymbol{r}) + (w_s(\boldsymbol{r}) + H(\boldsymbol{r}))\phi_s(\boldsymbol{r})] \\ &+ \frac{1}{V}\int d\boldsymbol{r}\xi(\boldsymbol{r})[\phi_h(\boldsymbol{r}) + \phi_t(\boldsymbol{r}) + \phi_s(\boldsymbol{r}) - \phi_0(\boldsymbol{r})]. \quad (1)\end{aligned}$$

Here, the local volume fractions of A (head) and B (tail) segments of the amphiphiles are given by $\phi_h(\boldsymbol{r})$ and $\phi_t(\boldsymbol{r})$. Likewise, $\phi_s(\boldsymbol{r})$ is the local concentration of homopolymer solvent. The average volume fractions of amphiphilic copolymer and solvent homopolymer are $\bar{\phi}_a$ and $\bar{\phi}_s$, respectively. The $w_h(\boldsymbol{r})$, $w_t(\boldsymbol{r})$, and $w_s(\boldsymbol{r})$ are the conjugate fields to the local volume fractions $\phi_h(\boldsymbol{r})$, $\phi_t(\boldsymbol{r})$, and $\phi_s(\boldsymbol{r})$, respectively, in a space point $\boldsymbol{r}$. The k_B is the Boltzmann constant, and T is the absolute temperature. The hydrophobic and hydrophilic monomers interact with a local Flory–Huggins interaction repulsion parameter of strength χ, with a choice $\chi N = 30$. The $\xi(\boldsymbol{r})$ is the Lagrange multiplier which enforces the incompressibility condition of the system. The Q_s and Q_a are the single chain partition functions of the solvent and amphiphile molecules subjected to the above fields. The V is the total volume of the system.

The surface of the square-shaped particle is hard and impenetrable. The total segment density in the vicinity of its surface drops to zero in a boundary region of width ε according to[39–41]

$$\phi_0(x,y) = \begin{cases} 0, & \text{inside the square,} \\ \frac{1}{2}\left\{1 - \cos\left[\frac{\pi(x - L/2)}{\varepsilon}\right]\right\}, & L/2 \le |x| \le L/2 + \varepsilon, \quad |y| \le L/2 + \varepsilon, \\ \frac{1}{2}\left\{1 - \cos\left[\frac{\pi(y - L/2)}{\varepsilon}\right]\right\}, & L/2 \le |y| \le L/2 + \varepsilon, \quad |x| \le L/2 + \varepsilon, \\ 1, & \text{else,} \end{cases} \quad (2)$$

where ε is chosen much smaller than R_g, the polymer radius of gyration, and L is the side length of the square-shaped particle.

For simplicity, the surfaces of the nanoparticles are neutral. Within the well established SCFT, the boundary conditions are needed. At the boundary on the particle, because the hard particle surface and polymer cannot cross the boundary, the Dirichlet condition is used, that is to say, the propagator q in diffusion equation of SCFT theory[42] is enforced as $q(\boldsymbol{r}, \boldsymbol{r}', s) = 0$, at surfaces of the square-shaped particle. For the four boundaries of our simulation box, the Neumann condition is used, which are defined for the propagator q in the discretised equation as, $q(0, j, s) = q(2, j, s)$ and $q(N_x + 1, j, s) = q(N_x - 1, j, s)$.

We focus on the interfacial confinement effect on the copolymer morphology. Therefore, initially, the copolymer is confined in the vicinity of the square-shaped particle by an applied field $H(\boldsymbol{r})$ according to

$$H(\boldsymbol{r}) = \begin{cases} 0, & \text{inside the square,} \\ H_0\left\{1 - \cos\left[\frac{\pi(x - L/2)}{\varepsilon}\right]\right\}, & L/2 \le |x| \le L/2 + \varepsilon, \quad |y| \le L/2 + \varepsilon, \\ H_0\left\{1 - \cos\left[\frac{\pi(y - L/2)}{\varepsilon}\right]\right\}, & L/2 \le |y| \le L/2 + \varepsilon, \quad |x| \le L/2 + \varepsilon, \\ 0, & \text{else.} \end{cases} \quad (3)$$

The calculations use an initial random distribution of concentration with a small fluctuation amplitude to ensure that the observed morphologies are independent of the initial condition. After several computational turns, the copolymer completely distributes around the particle, the field $H(\boldsymbol{r})$ is then cancelled.[25,40,43,44] The simulation goes on until the phase patterns are stable. All the simulations are repeated by using different random numbers to guarantee that the observed structure is not artifacts. The applied field $H(\boldsymbol{r})$ makes it easier to access more complex metastable structures. In our calculation, H_0 is chosen to be slightly larger than the field $w(\boldsymbol{r})$ in the equilibrium state. The purpose of H is only to drive the copolymer distribution near the square-shaped particle. Many other H with different amplitudes are also used, and no effect to the final stable morphology is found. All the figures of morphologies in the paper are with the same size $20 \times 20R_g$. The system is large enough to avoid the effect of boundary condition on the morphologies of the copolymer.

3. Results

After the impressible condition $\phi_0(\boldsymbol{r}) \leq 0.0001$ satisfied, the system achieves equilibrium. The assembly morphology of the copolymer in the interface has complex geometries. For homopolymer with the same segment length of 100, we choose three different species of copolymer: (20/80), (30/70), and (40/60). Here, the symbol (20/80) denotes the copolymer chain with a hydrophilic segment length of 20 and a hydrophobic segment length of 80. These systems will predict the probable morphology transformations of vesicles and micelles. The corresponding phase diagrams of copolymer assembly are shown in Fig. 1, based on the parameters of copolymer volume fraction f and the side length L of square-shaped particle. To form an interface, the homopolymer are all restricted in the peripheral region of the system. Hence, these structures are all protected by monolayers on their periphery, out of which are the homopolymer (i.e., poor solvents).

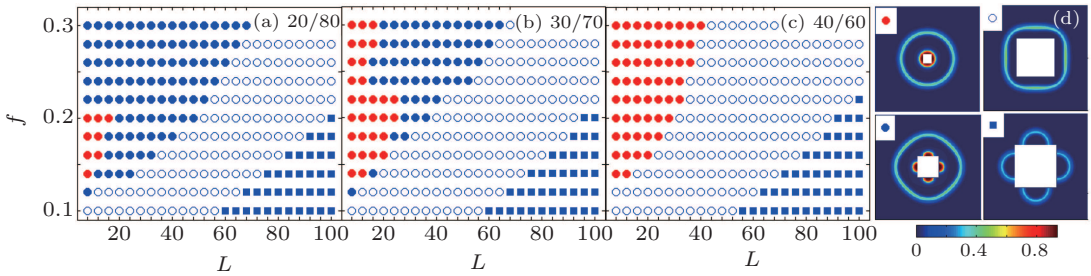


Fig. 1. (color online) The phase diagrams for copolymer with respect to volume fraction f and side length L of the square-shaped particles. The three phase figures are for copolymers (a): 20/80, (b) 30/70, and (c) 40/60. Four phase regions are shown by (i) red filled circles (denoting vesicles with particles in the core), (ii) blue filled circles (denoting combined structures with outer monolayer and inner inverted micelle pieces), (iii) hollow circles (denoting micelles with particles in the core), and (iv) blue filled squares (denoting micelle pieces). They represent four different morphologies in panel (d), respectively.

All the morphologies are classified as four types of structures, corresponding to the four figures in Fig. 1(d): (i) vesicles enclosing particles in the core (represented by red filled circles); (ii) combined structures with outer monolayers and inner inverted micelle pieces (denoted by blue filled circles); (iii) micelles with particles in the core (represented by hollow circles); and (iv) micelle pieces (denoted using blue filled squares). Generally speaking, the phase diagrams in Fig. 1 are roughly divided into three regions: (I) the upper left region is mainly vesicles and combined structures, with parameters of small L and large f; (II) the lower right region is pieces of micelles enclosing particles, with parameters of large L and small f; (III) the intermediate region is mainly micelles. From Fig. 1(a) to Fig. 1(c), the red dot area is gradually increased, because the vesicles prefer amphiphiles with large heads.

For convenience, each homopolymer and copolymer chain has the same segment length $N = 100$. Figure 2 demonstrates the assembly morphologies of the (20/80) copolymer with $f = 0.18$, for different L. For small particles, such as $L = 12$ in Fig. 2(b1), a vesicle is formed with particles enclosed in the core. In fact, the behavior of these small square-shaped particles likes that of spherical particles. With the increment of particle size, the inner monolayer is successively broken into two pieces of inverted micelles (see $L = 16$ in Fig. 2(b2)), four pieces of inverted micelles ($L = 32$ in Fig. 2(b3)), and two pieces of inverted micelles ($L = 36$ in Fig. 2(b4)) again. For large particles with $L = 44$ in Fig. 2(b6), the amount of copolymer is not large enough to support both the outer monolayer and the inner inverted micelles. The inner inverted micelles disappear, and only the outer monolayer is left. When the side length is increased further with $L = 92$ in Fig. 2(b8), the outer monolayer is also broken into four pieces of micelles, which symmetrically distribute on the four sides of the square, like a beautiful flower.

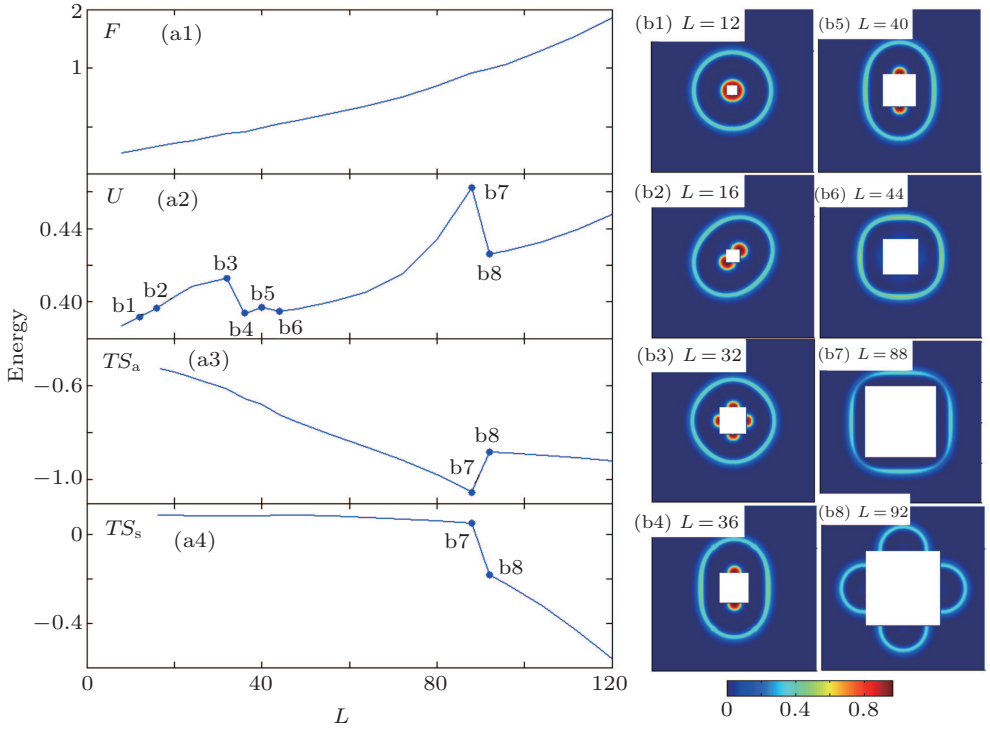


Fig. 2. (color online) (a1) The free energy F, (a2) the interfacial energy U, (a3) the amphiphile entropy S_a, and (a4) the solvent entropy S_s as functions of the side length L, for amphiphiles (20/80) with $f = 0.18$. The marks from panels (b1)–(b8) denote the 8 specific morphologies of the system, whose different structures have been shown in panels (b1)–(b8). The density distributions of the head parts of the amphiphiles, ϕ_h, are sequentially shown in panels (b1)–(b8), which correspond to the 8 states marked in the energy curves of the left column. The white squares schematically denote the square-shaped particles with different sizes.

In order to extract more physical insights from the morphology transformations, figures 2(a1)–2(a4) show the free energy F as functions of L. The three components of free energy: the interfacial energy U, the configurational entropy of amphiphile S_a, and solvent S_s are also obtained by separating the free energy as $F = U - T(S_a + S_s)$[28,39]

$$\frac{NU}{\rho_0 k_B T V} = \frac{1}{V}\int d\boldsymbol{r}[\chi N\phi_h(\boldsymbol{r})\phi_t(\boldsymbol{r}) + \chi N\phi_s(\boldsymbol{r})\phi_t(\boldsymbol{r})], \quad (4a)$$

$$\frac{NS_a}{\rho_0 k_B T V} = \frac{1}{V}\int d\boldsymbol{r}[w_h(\boldsymbol{r})\phi_h(\boldsymbol{r}) + w_t(\boldsymbol{r})\phi_t(\boldsymbol{r})] + \frac{\bar{\phi}_a}{\alpha}\ln\left(\frac{Q_a}{V\bar{\phi}_a}\right), \quad (4b)$$

$$\frac{NS_s}{\rho_0 k_B T V} = \frac{1}{V}\int d\boldsymbol{r}[w_s(\boldsymbol{r})\phi_s(\boldsymbol{r})] + \bar{\phi}_s\ln\left(\frac{Q_s}{V\bar{\phi}_s}\right). \quad (4c)$$

Clearly, with the increase of the particle size, the effective movement space of the copolymer is relatively enlarged. Hence, their conformational entropy is gradually increased. While for the homopolymer, because of there being no direct contact with the particle and no obvious confinement by the particle, their conformational entropy is little affected, and only slightly decreased. At $L = 92$ (Fig. 2(b8)), the complete outer monolayer bursts into four pieces. The space enclosed by the outer monolayer is also separated into four small spaces, which are independent of each other. It causes the sudden decrease of copolymer entropy and the sharp increase of homopolymer entropy.

To a large extent, the interfacial energy U is proportional to the interfacial area. When the morphology suddenly changes a lot, the interfacial area is effectively decreased, which is accompanied by the sharp decrease in the U curve. For example, the inverted micelle islands suddenly decrease their number from 4 in Fig. 2(b3) to 2 in Fig. 2(b4), and the whole outer monolayer suddenly splits into 4 individual micelle pieces from Fig. 2(b7) to Fig. 2(b8). Other cases such as from Fig. 2(b4) to Fig. 2(b7), the outer monolayer is gradually stretched, and the interfacial area is obviously enlarged. This causes a gradual increase in the U curve. Both copolymer and homopolymer get more severely restricted by the enlargening particle, which causes the increment of the total entropy. The combined effect of the above interfacial energy and conformational entropy results in the monotonic increase of the free energy curve.

We will analyze the four kinds of structures in Fig. 1. The micelles are relatively simple with various shapes, such as spherical (Fig. 2(b6)), elliptical (Fig. 3(b)), square (Fig. 4(c)), and cross-linked (Figs. 4(a) and 4(b)). As for the micelle pieces, the most common shapes are the four petal-shaped (Fig. 2(b8)) and two petal-shaped structures (Fig. 3(c)). The most complex morphology is the combined structure formed by outer monolayer and inner reverse micelles (see Figs. 2(b2)–2(b5), 3(a), and Fig. 5). There are often even numbers of inner inverted micelles, such as 6, 4, and 2. These

reverse micelles like islands symmetrically surround the particle. The copolymer chains with smaller hydrophilic heads have more flexibility in the formation of complex structures. The morphology with one reverse micelle is only found in the (20/80) copolymer with $f = 0.12$ and $L = 16$. For the present parameters and our grid calculation method, the structure with an odd number of reverse micelles is very rare. Because, the side length of the particle has to change one grid for every calculation, while the change range of parameters for an odd number of inverted micelles is smaller than the grid step. There may be another reason why the structures with an odd number of reverse micelles are relatively more instable than those with an even number of reverse micelles.

It is a combined effect between the number of reverse micelles and their distributions around the square-shaped particle. These factors include the entropy loss of copolymer chains near the particle, the volume fraction and the structure parameter of copolymer chains.

In fact, all the assembly structures are very rich and interesting. It is, of course, a difficult exercise to identify these structures separately from each other. In addition, it is not necessary to distinguish all of them. As a typical example, we see Figs. 2(b2)–2(b5), 3(a), and 5, all the morphologies are classified as combined structures with outer monolayers and inner reverse micelles, but they exhibit various detailed structures. Figures 2(b6), 2(b7), 3(b), and 4 are all explained as micelles, despite their different shapes. Figures 2(b8) and 3(c) are known as structures of micelle pieces, despite their rich detailed information.

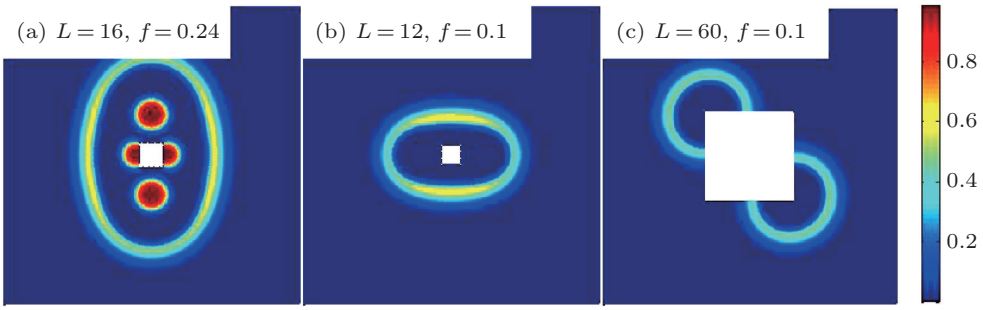


Fig. 3. (color online) The density distributions of the head part, ϕ_h, of the (30/70) amphiphiles, corresponding to different parameters in Fig. 1(b), for (a) $f = 0.24$, $L = 16$, (b) $f = 0.1$, $L = 12$, and (c) $f = 0.1$, $L = 60$. The white squares schematically denote the square-shaped particle with different sizes.

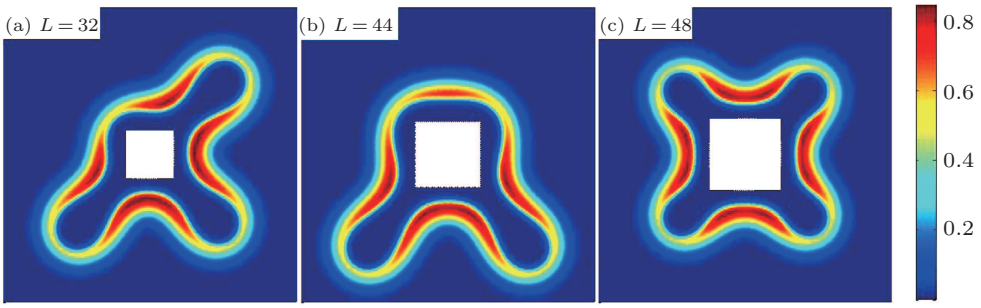


Fig. 4. (color online) The density distributions of the head part, ϕ_h, of the (40/60) amphiphiles, corresponding to different side lengths L ((a) $L = 32$, (b) $L = 44$, and (c) $L = 48$) in Fig. 1(c). All the figures are for the fixed volume fraction of copolymer $f = 0.26$. The white squares schematically denote the square-shaped particles with different sizes.

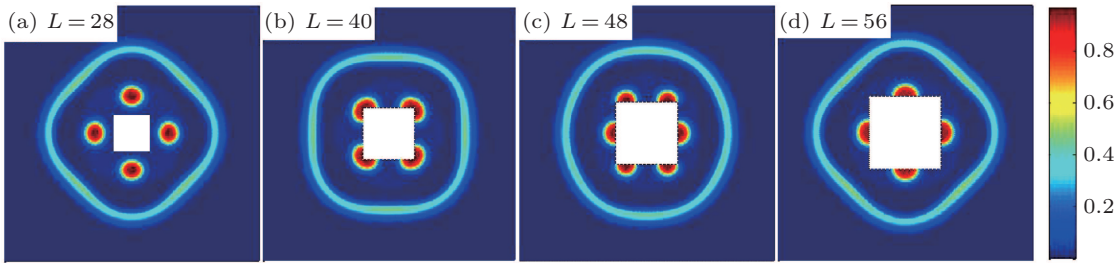


Fig. 5. (color online) The density distributions of the head part, ϕ_h, of the (20/80) amphiphiles with fixed volume fraction $f = 0.3$, corresponding to different side lengths L ((a) $L = 28$, (b) $L = 40$, (c) $L = 48$, and (d) $L = 56$) in Fig. 1(a). The white squares schematically denote the square-shaped particles with different sizes.

4. Conclusions

Controlling interfacial properties with polymers at the nanoscale offers exciting applications, such as in the fields of optics, biomaterials and corrosion. We have reported on the assembly morphology transformations of copolymer confined at the interface between the square-shaped particle and homopolymer melt. Here, we provide an interesting square-shaped confinement environment. The interface is formed by a hard particle surface and a soft homopolymer surface, not like in cylinder confinement[45,46] with two hard surfaces or in brush confinement with two soft surfaces.[47] The hard and soft surface confinements give rich structures of vesicles and micelles. The copolymer is often used as amphiphilic molecules and homopolymer as solvents in biomimetic fields.[10,48–51] Therefore, our results also have certain enlightening values for the morphology research of biomimetic membranes in complex confined environments, and for the soft confinement-induced morphologies of diblock copolymers.[23]

It should be interesting to examine the influences of other parameters on the morphology transformations, for example, the multicomponent effect of the amphiphiles, the different length effect of the amphiphiles and solvents chains. Here, the particle is with neutral surfaces. Other parameters that may be considered is the adsorption strength between the particle and amphiphile chains. Also, the distribution of reverse micelles around the sides or the corners of the square-shaped particle will be further explored in the following work.

References

[1] Wang Y, Hosta-Rigau L, Lomas H and Caruso F 2011 *Phys. Chem. Chem. Phys.* **13** 4782
[2] Agudo-Canalejo J and Lipowsky R 2015 *ACS Nano* **4** 3704
[3] Fredrickson G H and Helfand E 1987 *J. Chem. Phys.* **87** 697
[4] Hajduk D A, Takenouchi H, Hillmyer M A, Bates F S, Vigild M E and Almdal K 1997 *Macromolecules* **30** 3788
[5] Park C, Yoon J and Thomas E L 2003 *Polymer* **44** 6725
[6] Kim J U and O'Shaughnessy B 2006 *Macromolecules* **39** 41
[7] Yang R, Li B and Shi A C 2012 *Langmuir* **28** 1569
[8] Shi A C and Li B 2013 *Soft Matter* **9** 1398
[9] Yabu H, Higuchi T and Jinnai H 2014 *Soft Matter* **10** 2919
[10] Arora H, Du P, Tan K W, Hyun J K, Grazul J, Xin H L, Muller D A, Thompson M O and Wiesner U 2010 *Science* **330** 214
[11] Cerda J J, Sintes T and Chakrabarti A 2005 *Macromolecules* **38** 1469
[12] Yu B, Li B, Jin Q, Ding D and Shi A C 2007 *Macromolecules* **40** 9133
[13] Chen P, Liang H and Shi A C 2008 *Macromolecules* **41** 8938
[14] Huh J, Jung J Y, Lee J U, Cho H, Park S, Park C and Jo W H 2011 *ACS Nano* **5** 115
[15] Deng Z Y and Zhang L X 2015 *Acta Phys. Sin.* **64** 168201 (in Chinese)
[16] Hua Y F, Zhang D and Zhang L X 2015 *Acta Phys. Sin.* **64** 088201 (in Chinese)
[17] Cao X Z, Merlitz H, Sommer J U and Wu C X 2012 *Chin. Phys. B* **21** 118202
[18] Chantawansri T L, Bosse A W, Hexemer A, Ceniceros H D, Garca-Cervera C J, Kramer E J and Fredrickson G H 2007 *Phys. Rev. E* **75** 031802
[19] Xiang H, Shin K, Kim T, Moon S I, McCarthy T J and Russell T P 2005 *Macromolecules* **38** 1055
[20] Shin K, Xiang H, Moon S I, Kim T, McCarthy T J and Russell T P 2004 *Science* **306** 76
[21] Wu Y, Cheng G, Katsov K, Sides S W, Wang J, Tang J, Fredrickson G H, Moskovits M and Stucky G D 2004 *Nature Mat.* **3** 816
[22] Arkin H and Janke W 2012 *Phys. Rev. E* **85** 051802
[23] Chi P, Wang Z, Li B and Shi A C 2011 *Langmuir* **27** 11683
[24] Beer S, Mensink L I S and Kieviet B D 2016 *Macromolecules* **49** 1070
[25] Katsov K, Muller M and Schick M 2004 *Biophys. J.* **87** 3277
[26] Katsov K, Muller M and Schick M 2007 *Biophys. J.* **90** 915
[27] Lee J Y and Schick M 2007 *Biophys. J.* **92** 3938
[28] Thompson R B and Matsen M W 2000 *J. Chem. Phys.* **112** 6863
[29] Maniadis P, Lookman T, Kober E M and Rasmussen K O 2007 *Phys. Rev. Lett.* **99** 048302
[30] Drolet F and Fredrickson G H 1999 *Phys. Rev. Lett.* **83** 4317
[31] Duque D 2003 *J. Chem. Phys.* **119** 5701
[32] Martin J G and Gerhard G 2011 *Langmuir* **27** 3416
[33] Drolet F and Fredrickson G H 2001 *Macromolecules* **34** 5317
[34] Chen H Y and Fredrickson G H 2002 *J. Chem. Phys.* **116** 1137
[35] Matsen M W and Schick M 1994 *Phy. Rev. Lett.* **72** 2660
[36] Schmid F 1998 *J. Phys.: Condens. Matter* **10** 8105
[37] Matsen M W 2002 *J. Phys.: Condens. Matter* **14** R21
[38] Zhang Q Y 2009 *Chin. Phys. B* **18** 0658
[39] Matsen M W and Bates F S 1997 *J. Chem. Phys.* **106** 2436
[40] Lee J Y, Shou Z and Balazs A C 2003 *Phys. Rev. Lett.* **91** 136103
[41] Muller M and Binder K 2005 *J. Phys.: Condens. Matter* **17** S333
[42] Jaeup U K and Mark W M 2008 *Macromolecules* **41** 246
[43] Zhang Q Y and Ma Y Q 2006 *J. Chem. Phys.* **125** 164710
[44] Zhang Q Y and Ma Y Q 2006 *J. Phys. Chem. B* **110** 26279
[45] Yu B, Li B, Jin Q, Ding D and Shi A C 2011 *Soft Matter* **7** 10227
[46] Zuo Y, Wang G, Yu Y, Zuo C, Shi L and Wei J 2015 *Polymers* **7** 120
[47] Ren C L, Chen K and Ma Y Q 2005 *J. Chem. Phys.* **122** 154904
[48] Grubbs R B and Sun Z 2013 *Chem. Soc. Rev.* **42** 7436
[49] Zhu Y, Yang Q, Tong C, Li M and Yu X 2010 *Polymer* **51** 702
[50] He P, Li X, Kou D, Deng M and Liang H 2010 *J. Chem. Phys.* **132** 204905
[51] Antunes F E, Marques E F, Miguel M G and Lindman B 2009 *Adv. Coll. Inter. Sci.* **147** 18